The Plant Journal (2008) doi: 10.1111/j.1365-313X.2008.03460.x

Characterization of a sub-family of Arabidopsis genes with the SPX domain reveals their diverse functions in plant tolerance to phosphorus starvation

Ke Duan†, Keke Yi†, Lei Dang†, Hongjie Huang, Wei Wu and Ping Wu*

State Key Laboratory of Plant Physiology and Biochemistry, College of Life Science, Zhejiang University, Hangzhou 310058, China

Received 5 October 2007; revised 12 December 2007; accepted 7 February 2008.
*For correspondence (fax +86 571 88206617; e-mail clspwu@zju.edu.cn).
†These authors contributed equally to this work.

Summary

Four genes of Arabidopsis (At5g20150, At2g26660, At2g45130 and At5g15330) encoding no conservative region other than an SPX domain (SYG1, Pho81 and XPR1) were named *AtSPX1–AtSPX4*. The various subcellular localizations of their GFP fusion proteins implied function variations for the four genes. Phosphate starvation strongly induced expression of *AtSPX1* and *AtSPX3* with distinct dynamic patterns, while *AtSPX2* was weakly induced and *AtSPX4* was suppressed. Expression of the four *AtSPX* genes was reduced to different extents in the Arabidopsis *phr1* and *siz1* mutants under phosphate starvation, indicating that they are part of the phosphate-signaling network that involves SIZ1/PHR1. Over-expression of *AtSPX1* increased the transcript levels of *ACP5*, *RNS1* and *PAP2* under both phosphate-sufficient and phosphate-deficient conditions, suggesting a potential transcriptional regulation role of AtSPX1 in response to phosphate starvation. Partial repression of *AtSPX3* by RNA interference led to aggravated phosphate-deficiency symptoms, altered P allocation and enhanced expression of a subset od phosphate-responsive genes including *AtSPX1*. Our results indicate that both AtSPX1 and AtSPX3 play positive roles in plant adaptation to phosphate starvation, and AtSPX3 may have a negative feedback regulatory role in AtSPX1 response to phosphate starvation.

Keywords: Arabidopsis, phosphate starvation, SPX domain gene, gene expression, gene function.

Introduction

The essential macronutrient phosphorus (P) serves as a structural element for organic compounds, an intermediate for bio-energetic processes, and a component in signaling cascades (Poirier and Bucher, 2002). The chemical properties of P determine its low bioavailability in soils. To cope with low nutritional phosphate (P_i) availability, plants have evolved sophisticated metabolic and developmental strategies to facilitate P_i acquisition and remobilization. Plants may increase P_i uptake by expanding their root system to achieve a higher absorption surface, and enhance P_i uptake efficiency by organic anion excretion and elevated expression of transporters and acid phosphatase (Abel *et al.*, 2002). Although knowledge of P_i uptake and the P_i-signaling system has increased recently (Bari *et al.*, 2006; Chen *et al.*, 2007; Chiou *et al.*, 2006; Devaiah *et al.*, 2007a,b; Fujii *et al.*, 2005; Shin *et al.*, 2006), the molecular network underlying plant adaptation to P_i starvation is still to be elucidated.

The hydrophilic and poorly conserved SPX domain (SYG1/Pho81/XPR1) is found at the N-termini of various proteins, particularly signal transduction proteins (Barabote *et al.*, 2006). There are genes harboring the SPX domain in all major eukaryotic kingdoms. SYG1 inhibits transduction of the mating pheromone signal in yeast via direct binding to the G-protein β-subunit (Spain *et al.*, 1995). PHO81, the putative sensor of P_i levels in yeast, is a cyclin-dependent kinase (CDK) inhibitor that is induced by P_i starvation, interacting with cyclin PHO80 to repress the activity of CDK PHO85, thus promoting the expression of PHO2/PHO4 and enhancing yeast tolerance to P_i starvation (Lenburg and O'Shea, 1996). The human protein XPR1 functions as a cell-surface receptor for xenotropic and polytropic retroviruses,

T P J 3 4 6 0 B
Journal Name Manuscript No.
Dispatch: 10.3.08 Journal: TPJ CE: Bharathy
Author Received: No. of pages: 11 PE: Aswini

and is probably also involved in G-protein-mediated signaling (Battini *et al.*, 1999).

Most identified plant SPX gene products are involved in responses to environmental cues or internal regulation of nutrition homeostasis. Barley IDS4 (iron-deficiency specific clone 4) contains part of the SPX domain and is preferentially expressed in Fe-deficient roots (Nakanishi *et al.*, 1993). Arabidopsis PHO1, harboring both SPX and EXS domains, plays a role in loading root P_i into the xylem vessels, and loss of PHO1 function in *pho1* mutants results in P_i deficiency in above-ground tissues (Hamburger *et al.*, 2002; Poirier *et al.*, 1991). A PHO1 homolog in Arabidopsis may have a similar role in P_i loading and signaling (Wang *et al.*, 2004). The product of the tomato *IDS4-like* gene interacts with the leucine zipper domain of a hypoxia-induced transcription factor involved in the low-oxygen response (Sell and Hehl, 2005). Homologous to yeast SYG1, the Arabidopsis SHORT HYPOCOTYL UNDER BLUE 1 (SHB1) protein acts in cryptochrome signaling and possible phytochrome-mediated light responses (Kang and Ni, 2006).

The Arabidopsis genome encodes 20 genes with the SPX domain, grouped into four sub-families. Three sub-families, with a total of 16 members, encode proteins with the SPX domain and an extra conservative domain, including *AtPHO1*, which is involved in regulation of P_i homeostasis in Arabidopsis (Wang *et al.*, 2004). The other four members (At5g20150, At2g26660, At2g45130 and At5g15330) form a unique sub-family encoding proteins of about 300 amino acids in size, with no conservative region of the Pfam-A type other than the SPX domain. Here these four genes are named sequentially as *AtSPX1–AtSXP4*. To probe their potential role in plant responses to P_i signaling, we characterized their expression profiles and localization of their GFP fusions. Intriguing differences were revealed in their dynamic expression patterns under P_i deficiency and in the localization of the GFP fusions. Relevant over-expression materials and T-DNA insertion mutants or RNAi materials were subsequently generated, and phenotypes were investigated under P_i deficiency or P_i sufficiency. Gene expression patterns and plant developmental phenotypes in the corresponding genetic materials highlighted the evolutionary diversification in their biological roles. Our results suggest involvement of *AtSPX1* in transcriptional regulation of P_i-responsive genes, and of *AtSPX3* in potential negative feedback regulation of the P_i-signaling network.

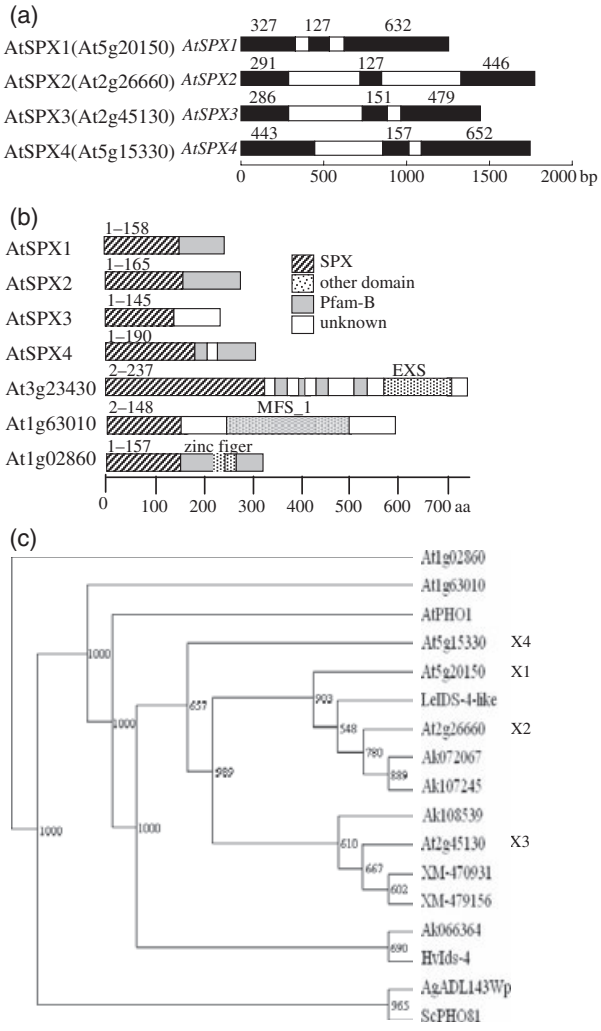

Figure 1. Structure and homology of *AtSPX1–4*.
(a) Intron (white box) and exon (black box) organization of *AtSPX1–4*. The numbers indicate the length in base pairs (bp) of the corresponding exon.
(b) Modular structure of Arabidopsis proteins encompassing a SPX domain. The numbers indicate the amino acid ranges of the SPX domain (Pfam-A) spanned. Pfam-B, less conservative; unknown, non-conservative.
(c) Phylogenetic tree of AtSPX1–4 and homologous proteins from other eukaryotes. In addition to AtSPX1–4, other Arabidopsis SPX proteins shown are: AtPHO1 (At3g23430) with an extra EXS domain, At1g63010 with an extra transporter-like domain (MFS_1), and At1g02860 with a zinc finger. Other proteins include tomato (Le) IDS4-like, barley HvIds4, cotton (Ag) ADL143Wp and yeast (Sc) PHO81, as well as six rice SPX proteins AK072067, AK107245, AK108539, XM-470931, XM-479156 and AK066364. The tree was created using the ClustalX program (http://www.ebi.ac.uk/clustalw/) (Jeanmougin and Thompson, 1998).

Results

Structural and homologous characterization of four SPX domain genes

The four *AtSPX* genes encoding no conserved region except for a SPX domain are referred to as *AtSPX1* (At5g20150), *AtSPX2* (At2g26660), *AtSPX3* (At2g45130) and *AtSPX4* (At5g15330). The *AtSPX* genes all have three exons and two introns (Figure 1a). The position and size of the three exons are fairly well conserved, with the SPX coding region mainly spanning the first two exons. Pairwise comparison reveals that *AtSPX1* and *AtSPX2* share more structural features, while *AtSPX3* is similar to *AtSPX4*. The SPX domain in *AtSPX1* and *AtSPX2* spans the first two exons to the 5′ end of

the third exon. Thus, the greatest divergence in the structure of the four genes is the relative lengths of the intron and exon ranges spanned by the SPX domain.

Their deduced proteins are similar lengths (245–318 amino acids) with 41–72% similarity (Figure 1b). Analysis of their tripartite SPX domain revealed 50–77% similarity of amino acids in the entire SPX domain, but >90% in each sub-domain, with the third sub-domain being the most conserved (Figure S1). Representative genes that are homologous to the *AtSPX* genes are shown in Figure 1(c), and their amino acid sequence alignment analysis is shown in Figure S2. *AtSPX1–4* are more homologous to SPX genes from other plant species that to other Arabidopsis SPX genes.

Subcellular localization of the AtSPX proteins

No signal peptide has been predicted for the deduced AtSPX proteins, except for a *bipartite nuclear-targeting sequence* KRLKLIGSKTADRPVKR from amino acids 30–46 in AtSPX1 (http://ca.expasy.org/prosite/PROSITE). C-terminal GFP fusions driven by CaMV 35S were used for visualization of AtSPX localization. Expression clones were transformed into onion epidermal cells for transient assay (Figure 2a,c,e,g). AtSPX1–GFP and AtSPX2–GFP were localized exclusively to the nucleus, while fluorescence of AtSPX4–GFP was detected in regions that included the cytoplasmic membrane. AtSPX3–GFP was present in onion cells as many fluorescent speckles in the cytoplasm. The peroxisome-localized RFP plasmid pCAMB-RFPPTS1 was co-transformed into onion cells with the AtSPX3–GFP plasmid, and partial overlapping of green and red fluorescence was observed (Figure S2).

Transgenic Arabidopsis materials were subsequently generated for the AtSPX–GFP fusion proteins. Stable expression of AtSPX2–GFP in Arabidopsis roots was localized to the same cellular location as in the transient assay (Figure 2d). Fluorescence of AtSPX4–GFP was found in the cytoplasmic membrane, and weak signals were observed in some intercellular membranous systems (Figure 2h). There was no obvious green fluorescence in transgenic seedlings harboring AtSPX1–GFP or AtSPX3–GFP constructs. Therefore, a transient expression assay was performed in Arabidopsis mesophyll protoplasts. AtSPX1–GFP was localized to the nuclei in Arabidopsis protoplasts as for onion cells (Figure 2b), consistent with the prediction by PROSITE. Fluorescence of AtSPX3–GFP partially overlapped with the auto-fluorescence of chlorophyll in the mesophyll protoplasts (Figure 2f). AtSPX3 may be localized in abundant intercellular membranous particles, including microbodies and chloroplasts.

Histochemical analysis for the AtSPX genes

To study the expression profiles of the *AtSPX* genes, the 1.5–2.0 kb promoter/5′ UTR region for each gene was amplified (designated AtSPX1p, AtSPX2p, AtSPX3p and AtSPX4p) and fused to β-glucuronidase (GUS) in pCambia1391Z and then transformed into Arabidopsis (Col).

Continuous GUS staining in young seedlings from germination revealed varied patterns (Figure 3a,b). AtSPX1p and AtSPX4p showed strong staining in cotyledons and

LOW RESOLUTION COLOUR FIG

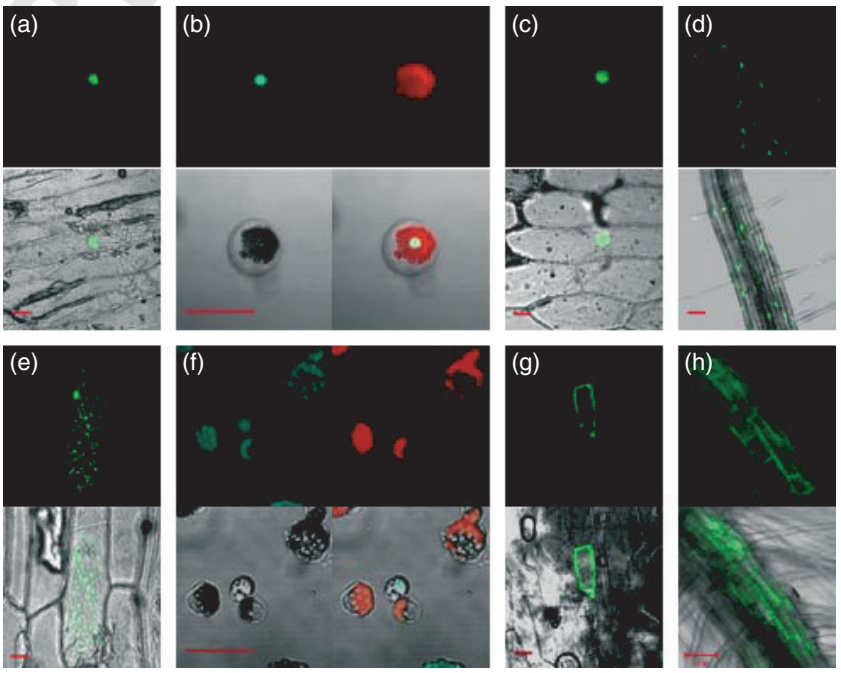

Figure 2. Expression of CaMV 35S::*AtSPX*–GFP fusion genes in onion and Arabidopsis.
Expression of AtSPX1–GFP in onion cells (a) and Arabidopsis mesophyll protoplasts (b), of AtSPX2–GFP in onion cells (c) and Arabidopsis root (d), of AtSPX3–GFP in onion cells (e) and Arabidopsis mesophyll protoplasts (f), and of AtSPX4–GFP in onion cells (g) and Arabidopsis root (h). The red in (b) and (f) is auto-fluorescence of chlorophyll. The lower part of each picture is the merged image or bright-field image. Bar = 50 μm.

LOW RESOLUTION COLOUR FIG

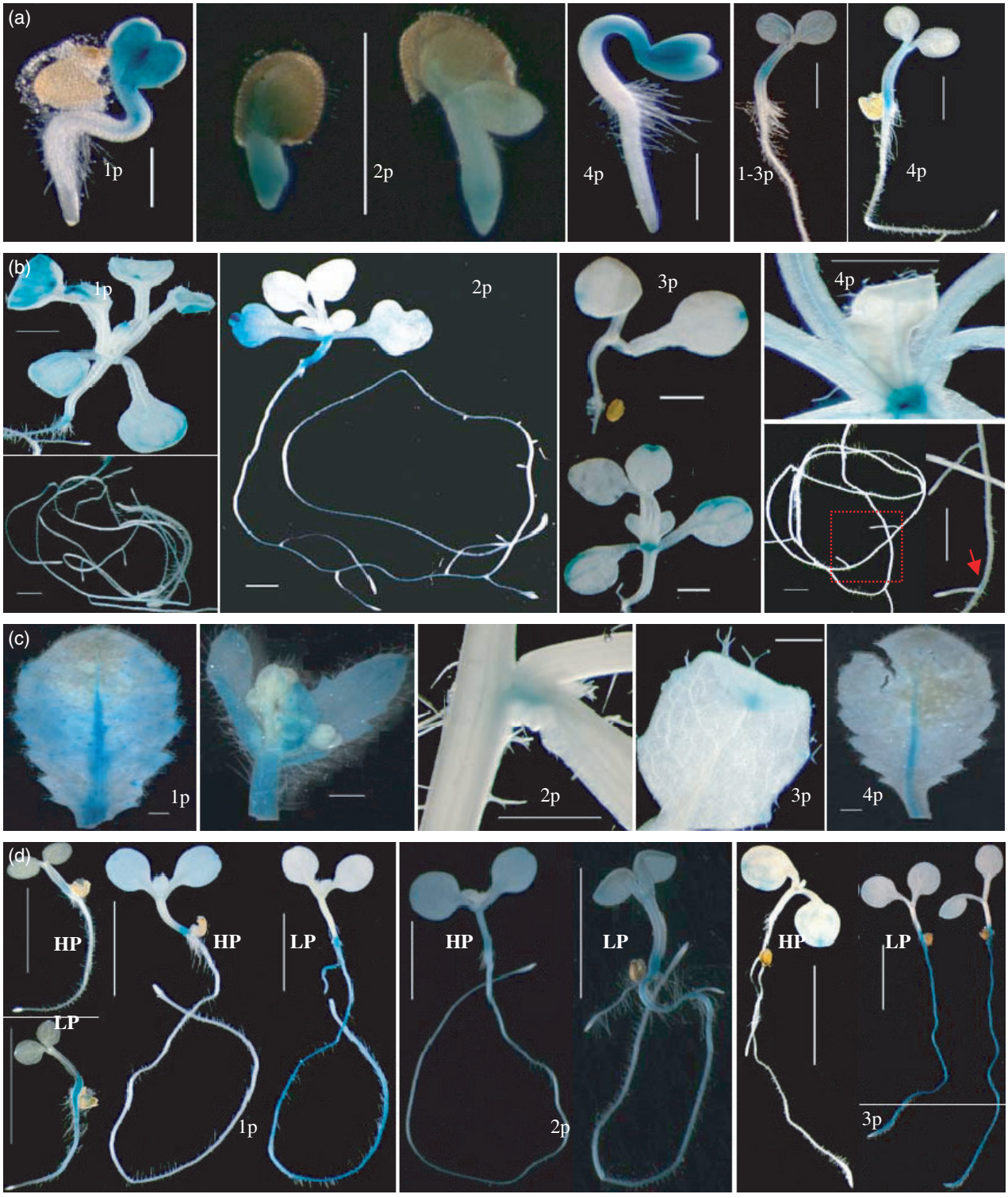

Figure 3. GUS staining of transgenic Arabidopsis harboring *AtSPX* promoter–GUS fusions.
GUS fusions of *AtSPX1–4* promoters are marked '1p'–'4p', respectively. (a) From germination to 4 DAG. Bar = 0.5 mm for seeds, 1 mm for young seedlings. (b) From 7–14 DAG: distinct activities are seen in root, leaf veins and the shoot apical meristem. Bar = 1 mm. (c) Mature plants: various staining patterns in leaf and stem. Bar = 1 mm. (d) GUS staining under high P_i (HP, 1 mM $NH_4H_2PO_4$) or low P_i (LP, 15 μM $NH_4H_2PO_4$). AtSPX1p was induced by P_i deficiency at 3 and 7 DAG; AtSPX2p was moderately induced at 7 DAG; AtSPX3p was intensively induced at 7 DAG. Bar = 3 mm.

hypocotyls, while AtSPX2p showed moderate staining in radicles. AtSPX3p showed no activity during early germination, and the first staining observed was in hypocotyls 5 days after germination (DAG). The full opening of cotyledons was followed by decreased promoter activity in cotyledons and radicles, but increased in hypocotyls for AtSPX1p, AtSPX12p and AtSPX14p. Later, there was obvious staining for AtSPX1p in leaf veins, preferentially in the abaxial region of leaf blades, and also in the branching regions of primary and lateral roots (Figure 3b). AtSPX2p was active in cotyledons and roots on appearance of the first leaf. AtSPX3p–GUS staining was only observed in leaf veins and shoot apical meristems but not in root systems under optimal nutrition. AtSPX4p activity was high in shoot apical meristems and weak in lateral root initiation regions (vascular tissue).

In mature plants, AtSPX1p–GUS staining was observed in rosette leaves (veins and trichomes) and cauline leaves (Figure 3c). AtSPX2p–GUS activity was not found in leaves, but was seen in stems at branching of axillary shoots. Staining for AtSPX3p–GUS was only observed in the abaxial region of the leaf blade. AtSPX4p activity was evident in the main vein of rosette leaves. All promoters uniformly displayed activity in mature pollen grains, and the staining intensity was consistent with pollen activity following petal unfolding (Figure S3). Control plants transformed by pCambia1391Z without insertions showed weak GUS staining in the base of pistils, young siliques and flower stalks (data not shown).

Expression responses of the AtSPX *genes to P_i starvation*

To study the response of the *AtSPX* genes to P_i starvation, transgenic seeds harboring promoter–GUS fusions were germinated on media with various P_i concentrations. P_i starvation enhanced the expression of all AtSPXp–GUS fusions except AtSPX4p–GUS (Figure 3d). AtSPX1p activity was rapidly induced by P_i starvation, with detectable promotion at 3 DAG and to an even higher degree at 7 DAG. There were detectable increases in AtSPX2p and AtSPX3p activities at 5 DAG (data not shown), and AtSPX3p was most highly induced at 7 DAG.

Quantitative RT-PCR was subsequently performed (Figure 4a,b). P_i starvation for 1 day markedly increased *AtSPX1* transcript abundance, especially in roots. P_i starvation for 5 days led to notable expression enhancement of *AtSPX1–3*, with higher levels in roots than shoots. Re-supply of P_i for 1 day quickly decreased their abundance, especially of *AtSPX3* in roots. In contrast, P_i starvation for 1 day reduced the level of *AtSPX4* transcript to half that before treatment. Prolonged P_i deficiency did not affect *AtSPX4* transcription further, but re-supply of P_i for 1 day resulted in complete

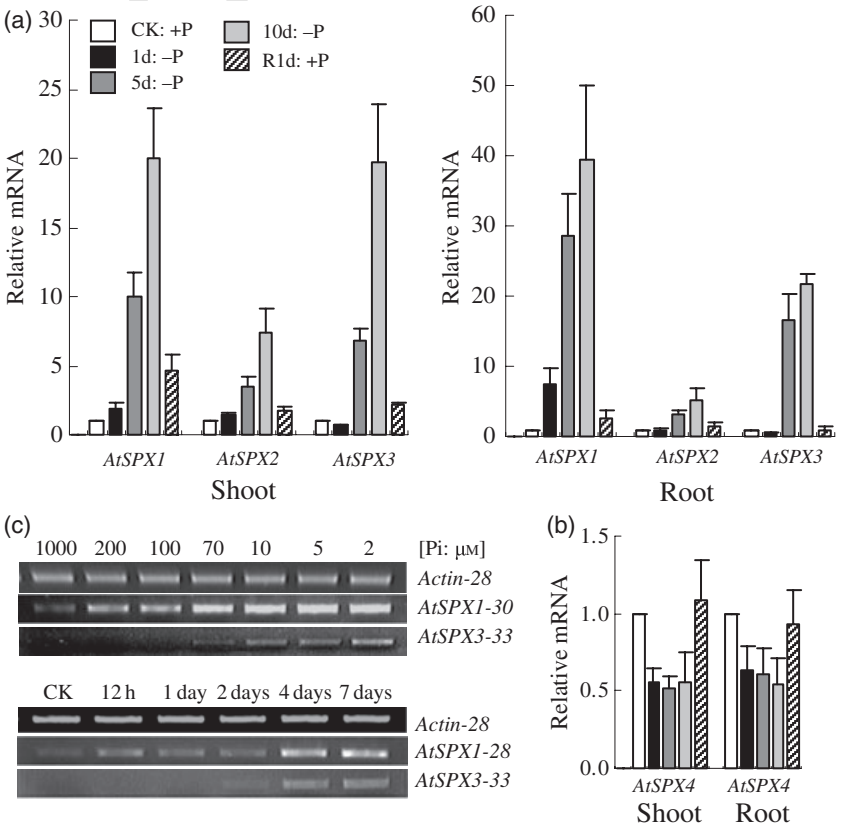

Figure 4. Responses of *AtSPX* genes to P_i starvation in Col.
(a) Quantitative RT-PCR analysis. Expression was relative to the transcript levels in shoots or roots under P_i-sufficient conditions (1 mM P_i). CK, P_i-sufficient; 1, 5 and 10 days, duration of P_i starvation (15 μM) (days); R1d, 10 days of P_i starvation followed by 1 day on P_i-sufficient substrate.
(b) Semi-quantitative RT-PCR analysis of AtSPX1 and AtSPX3. The dosage effects (1 week on media with varied P_i concentration, μM) and the dynamic influences of P_i starvation (2 μM P_i) on gene expression are shown in the upper and lower panels, respectively.

recovery. The results of semi-quantitative RT-PCR distinguished *AtSPX1* from *AtSPX3* (Figure 4c). *AtSPX1* was induced by one-week starvation on 200 μM P_i, and *AtSPX3* was induced by one week on 70 μM P_i. *AtSPX1* also responded more rapidly, with distinctly increased transcript levels after 12 h P_i starvation (2 μM P_i), while there was an obvious increase in *AtSPX3* transcripts only after 4 days of P_i starvation.

Transgenic plant analysis

For functional characterization, generation of over-expression materials for the *AtSPX* genes was paralleled by isolation of mutants or RNAi materials. Expression of the P_i starvation-inducible genes *ACP5*, *PAP2* and *RNS1* was enhanced in *AtSPX1*-over-expressing plants relative to the wild-type (WT). This expression enhancement was more significant under P_i sufficiency (Figure 5a,b) than under P_i deficiency. The 3–5-fold increased *AtSPX1* expression was paralleled by similar elevations of *ACP5* and *PAP2* expression in shoots, and a greater increase of *ACP5* expression in roots under P_i sufficiency. Under P_i starvation, *AtSPX1* expression was not so obviously changed, but the other three genes were clearly upregulated in shoots, and the expression of *RNS1* was clearly increased in roots. Together, these results indicate that AtSPX1 may be actively involved in P_i-signaling pathways by regulating the expression of the P_i-responsive genes *ACP5*, *PAP2* and *RNS1*.

The T-DNA insertion mutants SALK_039445, SALK_080503 and SALK_019826, corresponding to interruption of *AtSPX1*, *AtSPX2* and *AtSPX4*, respectively, were obtained from the Arabidopsis Biological Resource Center and propagated and validated for exact genome insertion and complete expression deletion. There were no obvious phenotypes for these mutants under either P_i sufficiency or deficiency. Because a T-DNA insertion mutant of *SPX3* was not available, an RNAi strategy was adopted and two *AtSPX3*-repressed lines were developed (Figure 6a). The *AtSPX3* RNAi plants presented no detectable phenotype under P_i sufficiency. *AtSPX1*, *AtSPX2* and *AtSPX4* were not significantly affected in *AtSPX3*-repressed lines under P_i sufficiency, suggesting specific interference on *AtSPX3* (Figure S4).

AtSPX3-repressed lines showed lowered plant tolerance to P_i starvation, including reduced root systems and impaired aerial parts (Figure 6b). The primary root elongation in *AtSPX3*-repressed lines was much reduced by P_i starvation compared to WT (Figure 6c). The concentration of P in the WT and *AtSPX3*-repressed lines were determined (Table 1). Total P (mg P per g dried plant) was significantly higher in shoots and lower in roots of the two lines Ri1 and Ri2 compared to that in WT. P_i concentration (mg P_i per g fresh plant) increased by >60% in the shoots of *AtSPX3*-repressed lines compared to WT. The P_i level in the roots was unchanged in Ri1, but increased in Ri2.

Relevant gene expression was analyzed to further understand the hypersensitive phenotype of the *AtSPX3*-repressed lines. The P_i-responsive genes examined comprise the TPS1/Mt4 family genes *IPS1* and *At4*, the Pht1 transporter family (nine members), the secreted phos-

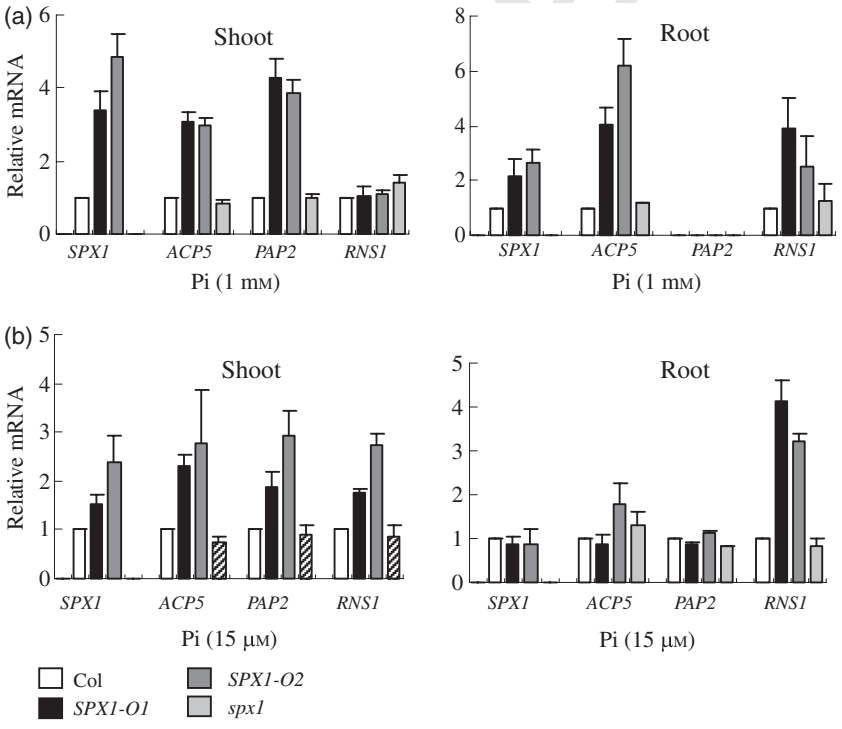

Figure 5. (a) Quantitative RT-PCR analysis of P_i starvation-responsive genes in Col, *AtSPX1*-over-expressing lines (*SPX1-O1* and *SPX1-O2*) and an *AtSPX1* mutant (SALK_039445), under P_i-sufficiency conditions (1 mM) at 10 DAG.
(b) Expression profiles of the same genes under P_i-starvation conditions (15 μM) at 10 DAG.

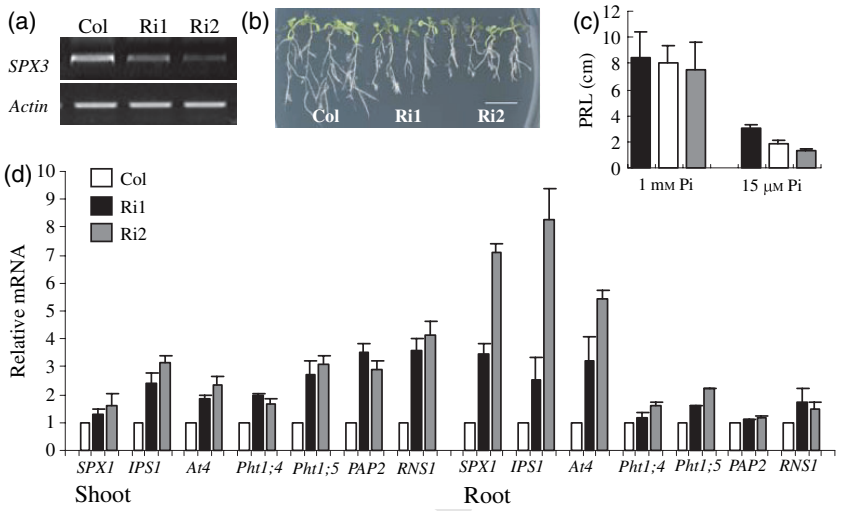

Figure 6. (a) Semi-quantitative RT-PCR analysis of *AtSPX3* in Col and transgenic plants. Plants grown under P_i deficiency (15 μM P_i) to 11 DAG were used for RNA analysis. Upper panel, 32 cycles for *AtSPX3* amplification; lower panel, 28 cycles for *Actin* amplification.
(b) Growth status of Col and *AtSPX3*-repressed lines (Ri1 and Ri2) under P_i deficiency (15 μM P_i) at 11 DAG. Bar = 1 cm.
(c) The primary root length (PRL) of WT and *AtSPX3*-repressed lines under P_i sufficiency (1 mM P_i) and P_i deficiency (15 μM P_i).
(d) Quantitative RT-PCR analysis for P_i-starvation-induced genes in *AtSPX3*-repressed lines. The genes shown are *AtSPX1*, *PAP2* (At1g66390), *RNS1* (At2g02990), *IPS1* (At3g09922), *At4* (At5g03545), *AtPht1;4* (At2g38940) and *AtPht1;5* (At2g32830).

Table 1 Total phosphorus (P) (mg g^{-1} DW) and inorganic phosphate (P_i) concentrations (mg g^{-1} FW) in *AtSPX3*-repressed lines (Ri1 and Ri2) and the wild-type (WT) grown on P_i-deficient medium (15 μM $NH_4H_2PO_4$)

	Tissue	WT	Ri1	Ri2
P	Shoot	17.65 ± 1.72	19.72 ± 1.32[a]	20.02 ± 0.75[a]
	Root	36.04 ± 3.05	32.72 ± 2.47[a]	28.02 ± 2.25[a]
P_i	Shoot	0.103 ± 0.02	0.166 ± 0.02[a]	0.174 ± 0.03[a]
	Root	0.379 ± 0.06	0.404 ± 0.03	0.522 ± 0.04[a]

Shoots and roots were sampled from 11-day-old seedlings. The values represent the means ± SE of two independent experiments (n = 8).
[a]Significant difference (P < 0.01) in means between WT and transgenic plants.

phatase *ACP5* gene, ribonuclease genes *RNS1* and *RNS2*, the anthocyanin synthesis regulator *PAP2* gene (production of anthocyanin pigment 2), and the other *AtSPX* genes. There were considerable alterations in expression of the genes (Figure 6d). Of the transporter family tested, only expression of *Pht1;4* (AtPT2, Pht4) and *Pht1;5* (Pht5) clearly increased in shoots. Similarly, *PAP2* and *RNS1* were markedly elevated in shoots of transgenic plants. *AtSPX1* showed prominent expression enhancement in roots but a weak increase in shoots. *IPS1* and *At4* were upregulated in whole plants, more markedly in roots than shoots.

The AtSPX family is involved in P_i-signaling pathways controlled by PHR1 and SIZ1

To determine whether the SPXs are involved in P_i-signaling pathways, we further investigated the expression of *AtSPX* genes in mutants including *pho1* (Wang *et al.*, 2004), *pho2* (Bari *et al.*, 2006), *phr1* (Rubio *et al.*, 2001) and *siz1* (Miura *et al.*, 2005). Expression of all *AtSPX* genes under P_i starvation was not obviously changed in *pho1* and *pho2* (data

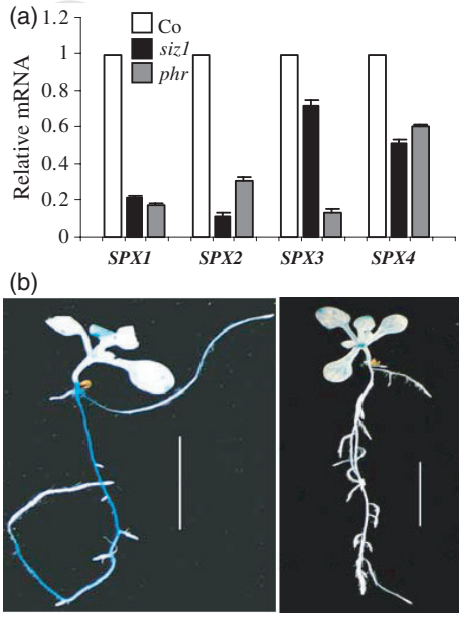

Figure 7. The AtSPX family is involved in P_i-signaling pathways.
(a) Quantitative RT-PCR analysis of *AtSPX* genes in Col and mutants under P_i starvation. Whole seedlings from P_i-sufficient medium at 7 DAG were transferred to P_i-deficient medium (15 μM $NH_4H_2PO_4$) for another one week, and then were harvested for RNA extraction.
(b) *AtSPX3p*–GUS staining in Col (left) and *phr1* (right) under P_i starvation at 10 DAG. Bar = 5 mm.

omitted), but was clearly impaired in *siz1* and *phr1* compared to WT (Figure 7a). *AtSPX1* was markedly repressed in *siz1* and *phr1*. *AtSPX2* expression was downregulated more in *siz1* than in *phr1*. *AtSPX4* expression was reduced to about half in *siz1*, with a mild decrease in *phr1*. *AtSPX3* expression was not significantly reduced in *siz1*, but was markedly downregulated to <10% in *phr1*. Consistent results were obtained for AtSPX3p–GUS staining in WT and *phr1*

(Figure 7b), strongly suggesting that expression of *AtSPX3* requires PHR1. These results suggest that AtSPX3 acts downstream of PHR1, while AtSPX1 and AtSPX2 have both PHR1 and SIZ1 as upstream regulators in P_i signaling.

Discussion

The *AtSPX* genes are highly homologous to each other in structure and sequence, but a subcellular localization assay discriminated between them and hinted at functional diversification. Various expression patterns for these genes were observed in response to P_i starvation. This indicates that plant genes with the SPX domain have diverse functions.

The expression of *AtSPX1* was most rapidly induced by P_i starvation. The nuclear localization of *AtSPX1*–GFP in Arabidopsis mesophyll protoplasts suggests its involvement in the transcriptional control of gene expression in response to P_i starvation. *AtSPX1* over-expression increased the expression of the P_i-responsive genes *ACP5*, *RNS1* and *PAP2*. The S-like ribonuclease RNS1 and the acid phosphatase ACP5 are involved in P_i recycling (Bariola *et al.*, 1994; Olczak *et al.*, 2003; del Pozo *et al.*, 1999). The anthocyanin accumulation-enhancing gene PAP2 is involved in scavenging active oxygen species (Borevitz *et al.*, 2000; Nagata *et al.*, 2003). Therefore, AtSPX1 may be involved in transcriptional activation of genes related to P mobilization and scavenging of active oxygen species in response to P_i starvation. The expression levels of these P_i-starvation-inducible genes were not altered between the AtSPX1 knockout mutant and WT, indicating that induction of these genes by P_i starvation was not only controlled by AtSPX1, although data showed that AtSPX1 was under the control of AtPHR1. PHR1 is expected to have multiple functions in regulation of the P_i-signaling pathway.

RNAi of AtSPX3 results in a hypersensitive response to P_i starvation, followed by a significant decrease in total P allocation to roots and an increase of both total P and P_i in shoots. The *AtSPX3*-repressed plants were quite different from the reported P_i-starvation hypersensitive mutant *PDR2*, which shows systemic impaired growth (Ticconi *et al.*, 2004). The P_i-signaling-related genes *IPS1* (Martin *et al.*, 2000) and *At4* (Shin *et al.*, 2006), together with *AtSPX1*, showed more enhanced expression in roots than in shoots. The P_i-recycling-related genes *RNS1*, *Pht1;4* and *Pht1;5* (Mudge *et al.*, 2002) and the anthocyanin synthesis-related gene *PAP2* were more increased in shoots than roots. These changes in gene expression were consistent with more severe P deficiency in roots and improved P remobilization in transgenic interfering plants compared to WT. This result implies that AtSPX3 has a positive role in plant adaptation to P_i starvation and is involved in negative feedback control of a subset of P_i marker genes. Our results reinforced the hypotheses that P_i-starvation-induced genes are under negative regulation, and the long-distance systemic signals controlling the P_i-starvation responses are dependent on whole-plant P_i status via negative modulation (Martin *et al.*, 2000; Mukatira *et al.*, 2001; Shin *et al.*, 2006). However, links between AtSPX3 and P_i signaling have not been established.

Recently, bioinformatic approaches have identified SPX domains in transport homologs of the divalent anion:Na^+ symporter family within the ion transporter superfamily (Barabote *et al.*, 2006). As signal reception is one of the few non-transport functions that transport homologs have acquired over evolutionary time (Pinson *et al.*, 2004), it is possible that most studied SPX proteins, such as SYG1 and PHO81, are involved in signal transduction. If it is supposed that the SPX domain functions as a sensor for P_i level in plants as it does for yeasts (Lenburg and O'Shea, 1996; Mouillon and Persson, 2006), the expression patterns and phenotypes shown here promote the hypothesis that AtSPX3 may have a role in sensing internal P_i deficiency, and AtSPX1 in sensing external P_i deficiency, both of which need to be further determined.

Figure 8 shows a scheme indicating the involvement of the AtSPX proteins in P_i-signaling pathways and their potential connections with some known components. PHR1, the MYB transcription factor, acts as a central factor that contributes to downstream P_i signaling by regulating the expression of a wide range of P_i-responsive genes (Rubio *et al.*, 2001), including at least three of the four *AtSPX* genes. The transduction of P_i-starvation signals to PHR1 relies on the SUMO E3 ligase SIZ1 (Miura *et al.*, 2005). *AtSPX1* positively regulates the expression of the P_i-starva-

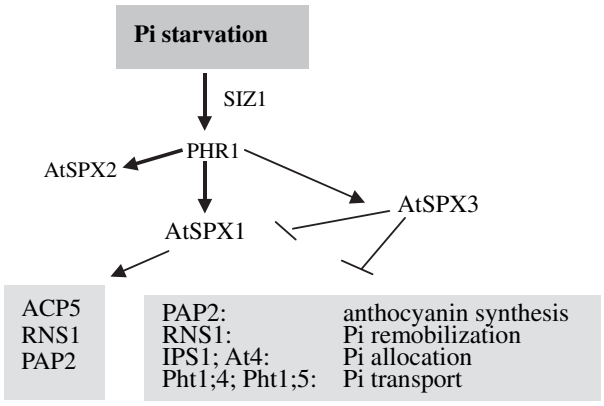

Figure 8. A suggested model for AtSPX involvement in P_i-signaling pathways.
PHR1 is essential for inducing expression of AtSPX1–3 under P_i starvation. SIZ1, upstream of PHR1, is important for *AtSPX1* and *AtSPX2* expression (thick line), but not for *AtSPX3* expression. *AtSPX1* activates the expression of *ACP5*, *PAP2* and *RNS1* via interaction with uncharacterized transcription factor(s). *AtSPX3*, acting downstream of PHR1, exerts negative feedback regulation of AtSPX1 and other factor(s) upstream of PHR1. *AtSPX3* repression results in upregulation of several P_i-responsive genes, including *AtSPX1*, *RNS1*, *PAP2*, *IPS1*, *At4*, *AtPht1;4* and *AtPht1;5*. Arrowheads show positive regulation; flat-ended lines show negative regulation.

tion-responsive genes *ACP5*, *PAP2* and *RNS1*. AtSPX3, acting downstream of PHR1, may exert negative feedback regulation on uncharacterized factors upstream of PHR1. AtSPX3 may also exert negative regulation on *AtSPX1* and six other genes, some of which are responsive to P_i starvation earlier than *AtSPX3*. The P_i-signaling pathways that AtSPX3 is involved in may also include microRNA regulation, as this vital factor for P_i homeostasis controls At4 expression (Bari *et al.*, 2006; Chiou *et al.*, 2006; Fujii *et al.*, 2005; Shin *et al.*, 2006).

Previous studies have suggested that the SPX domain is most likely a domain for protein interaction (Kang and Ni, 2006), and the tomato IDS4-like protein interacts with a leucine zipper transcription factor (Sell and Hehl, 2005). Thus, the AtSPX family may perform their functions via direct protein binding for signal transduction. The molecular links described here may advance our understanding of the P_i-signaling pathway.

Experimental procedures

Plant growth

Wild type (Col-0) and transgenic seeds were surface-sterilized with 10% commercial bleach in 100% ethanol for 10 min, followed by several washes with 95% ethanol. All the plant media used here have been described previously (Ma *et al.*, 2001). Agar B (0.7%) (Sangon Co. Ltd) was added to the media with a background P_i concentration of 1–2 μM. For expression profiling, seedlings germinated on normal medium (1 mM $NH_4H_2PO_4$) were transferred once at 7 DAG to fresh medium, partially or completely replacing $NH_4H_2PO_4$ with $(NH_4)_2SO_4$. For phenotype analysis, a direct seeding strategy was adopted on media with varying P_i. Plates were sealed with parafilm and placed vertically in a growth cabinet (Percival Scientific), with a 16 h light/8 h dark cycle, 150 μmol m^{-2} sec^{-1} photon flux density, and a constant temperature of 21.5°C.

Subcellular localization analysis

Full-length cDNA clones for the *AtSPX* genes were obtained from RIKEN BRC (pda07597 for AtSPX1, pda03041 for AtSPX4), the Arabidopsis Biological Resource Center (U68223 for AtSPX3) or directly amplified from Arabidopsis root cDNAs (for AtSPX2). pCambia1300 was modified in the our laboratory by introducing the CaMV 35S promoter between *Eco*RI and *Sac*I, and a *nos* terminator between *Pst*I and *Hin*dIII), and hereafter is referred as pCambia1300-mod. Full-length *mgfp4* with additional *Spe*I and *Sal*I recognition sites was amplified from pBIN121 and digested with *Spe*I and *Sal*I; full-length cDNAs before the stop codon of AtSPX1, AtSPX2 and AtSPX4 were amplified using the primer sets shown in Table S1 and digested with *Bam*HI and *Spe*I. The purified GFP and gene fragments were synchronously introduced into pCambia1300-mod linearized with *Bam*HI and *Sal*I. The resultant constructs were confirmed by PCR and restriction analysis. For the AtSPX3–GFP fusion construct, the full-length gene before the stop codon was amplified (using the primers shown in Table S1) and digested with *Bgl*II. This fragment was then transferred to the *Bgl*II site of pCambia-1302. The resultant vector with correct insertion orientation was identified by restriction analysis.

All the GFP fusion constructs, together with original pCambia-1302, pBIN121 and pCAMB-RFPPTS1, were transiently expressed in onion epidermal cells using the Bio-Rad biolistic PDS-1000/He system (http://www.bio-rad.com/), performed essentially as described previously (Varagona *et al.*, 1992). As for the transient expression assay in Arabidopsis cells, the mesophyll protoplasts were transformed by the PEG method (Sheen, 2001). For stable expression of GFP fusions, wild-type Col plants were transformed using the floral-dip method (Clough and Bent, 1998). The material used for GFP observation was the primary root of transgenic seedlings germinated on optimal medium for 5 days. The GFP fluorescence was imaged using a Carl Zeiss laser scanning system LSM510 (http://www.zeiss.com/).

Promoter–GUS constructs and histochemical analysis

The promoter 5′ UTR regions of the *AtSPX* genes were amplified from genomic DNA of Col using the primer pairs shown in Table S2. PCR products were first cloned into the pUCm-T vector (Shenerg Biocolor Co. Ltd) and sequenced for confirmation. Promoter fragments with correct insertion orientation were then transferred from pUCm-T to the expression vector pCambia1391Z between the cloning sites shown in Table S2. The resultant promoter–GUS constructs and the original pCambia1391Z were transformed into Col. Histochemical GUS staining was performed as described previously (Jefferson *et al.*, 1987). To study the promoter activity in response to to P_i starvation, transgenic seeds were directly germinated on P_i-replete (1 mM) or P_i-deficient (15 μM) media, and analyzed at 1, 3, 5 and 7 DAG.

Over-expression of AtSPX1

The over-expression construct was generated by inserting a full-length *AtSPX1* cDNA fragment into the binary vector pCambia1300-mod after the CaMV 35S promoter. The full-length *AtSPX1* from the 5′ UTR to the 3′ UTR was amplified from cDNA clone pda07597 using primers aaaaggtaccCATTCTCACTTAAGTTTCCCAG and aaaatctagaTTACATCAACTACAACACACC. The purified PCR product (1030 bp) was digested with *Kpn*I and *Xba*I, and subsequently cloned into pCambia1300-mod linearized with *Kpn*I and *Xba*I. Col plants were transformed using *Agrobacterium tumefaciens* EHA105, and transgenic plants were selected on hygromycin (20 mg l^{-1}) medium. T_3 progeny of two independent transgenic lines (T_1) were used for phenotype study and expression analysis.

RNAi of AtSPX3

pBluescript was first tailored by introducing the second intron (215 bp) of the *Phaseolus vulgaris* nitrite reductase (NIR) gene between the *Sph*I and *Pst*I sites to generate the pBSin vector. A 440 bp *AtSPX3* fragment was amplified using primers 5′-GTGGAATCTATTTTCGTCGGTT-3′ and 5′-CGCACATCTCTCGTATCCC-3′, and then cloned into pUCm-T. This fragment was twice transferred from pUCm-T into pBSin using the *Pst*I and *Bam*HI sites and the *Nsi*I and *Xho*I sites sequentially, giving rise to two copies of the insertion with reverse orientations separated by an intron (hairpin-type structure). The intron-interrupted 600 bp hairpin fragment (including 112–309 bp of the AtSPX3 open reading frame, corresponding to the coding region for SPX subdomain II and the adjoining spacing sequences) released from pBSin by *Nco*I digestion was blunted and cloned into pCambia-1301 linearized using *Sma*I. Restriction analysis using *Eco*RI and *Hin*dIII was performed to

confirm insertion of the hairpin loop into pCambia1301. The resultant expression vector was transformed into Col and more than 80 independent resistant T_0 lines were generated. Transformants confirmed as *AtSPX3*-deficient were further propagated. T_3 progeny of two independent transgenic lines (T_1) were used for phenotype analysis.

RNA isolation, cDNA preparation and RT-PCR

RNA was extracted from shoots, roots or whole seedlings at various stages as indicated. First-strand cDNAs were synthesized from total RNA using SuperScript™ II reverse transcriptase (Invitrogen, http://www.invitrogen.com/). Quantitative real-time PCR was performed using an ABI Prism 7000 sequence detection system (Applied Biosystems, http://www.appliedbiosystems.com/). Each 20 μl reaction contained 1 × SYBR Green master mix (Applied Biosystems), 0.5 μl cDNAs and 0.1 μl (20 μM) forward and reverse primers. The PCR conditions were as follows: 94°C for 2 min, followed by 40 cycles of 94°C for 15 sec, 58°C for 20 sec and 72°C for 30 sec. Fluorescence data were collected during the 72°C step and were analyzed using Sequence Detector version 1.7 software (Applied Biosystems). The amounts of cDNA template in each sample were normalized against that of actin. All primers for RT-PCR are shown in Table S3.

Measurement of P concentration in plants

Total phosphorus (P) was extracted from dried samples (30–50 mg) using sulfuric acid and hydrogen peroxide. Inorganic phosphate (P_i) in fresh samples (50–80 mg) was extracted using sulfuric acid. The P or P_i contents in plant sample solutions were analyzed 15 min after mixing with a malachite green reagent as described previously (Delhaize and Randall, 1995). The absorption values for the solutions at 650 nm were determined using a Spectroquant NOVA60 spectrophotometer. Eight samples were used for each genotype, and two independent experiments were performed.

Acknowledgements

We thank the ABRC (Arabidopsis Biological Resource Center, Ohio State University, USA) for cDNA clone U68223 (AtSPX3) and T-DNA insertion mutants SALK_039445, 080503 and 019826 (AtSPX1, AtSPX2 and AtSPX4), and RIKEN BRC (RIKEN BioResource Center, Japan) for cDNA clones pda07597 (AtSPX1) and pda03041 (AtSPX4). Dr Javier Paz-Ares (Centro Nacional de Biotecnología, Campus de Cantoblanco, Spain) and Dr Kenji Miura (Center for Plant Environmental Stress Physiology, Purdue University, West Lafayette, IN, USA) kindly provided homozygous seeds for the *phr1* and *siz1* mutants, respectively. We also thank Dr Yun Lin of the University of Illinois for generous provision of the pCAMB-RFPPTS1 vector. The work was supported by the National Key Basic Research Program of China (2005CB120900) and National Natural Science Foundation of China (30500310).

Supplementary Material

The following supplementary material is available for this article online:

Figure S1. Sequence alignment of the same homologues as in Figure 1c.

Figure S2. Transient expression of 35S::*AtSPX3*–GFP in onion cells using a particle bombardment assay.

Figure S3. GUS staining in pollen grains for all four *AtSPX* promoters.

Figure S4. Quantitative PCR analysis of *AtSPX1*, *AtSPX2* and *AtSPX4* transcript abundance in Col and of *AtSPX3* RNAi materials.

Table S1. Primer sets and vector information for generation of AtSPX–GFP fusion constructs.

Table S2. Primer sets and cloning sites (in p1391Z) for AtSPX promoter-driven GUS constructs.

Table S3. Primer sets used in RT-PCR analysis.

This material is available as part of the online article from http://www.blackwell-synergy.com.

Please note: Blackwell Publishing are not responsible for the content or functionality of any supplementary materials supplied by the authors. Any queries (other than missing material) should be directed to the corresponding author for the article.

References

Abel, S., Ticconi, C.A. and Delatorre, C.A. (2002) Phosphate sensing in higher plants. *Physiol. Plant.* **115**, 1–8.

Barabote, R.D., Tamang, D.G., Abeywardena, S.N. *et al.* (2006) Extra domains in secondary transport carriers and channel proteins. *Biochim. Biophys. Acta*, **1758**, 1557–1579.

Bari, R., Datt Pant, B., Stitt, M. and Scheible, W.R. (2006) PHO2, microRNA399, and PHR1 define a phosphate-signaling pathway in plants. *Plant Physiol.* **141**, 988–999.

Bariola, P.A., Howard, C.J., Taylor, C.B., Verburg, M.T., Jaglan, V.D. and Green, P.J. (1994) The Arabidopsis ribonuclease gene RNS1 is tightly controlled in response to phosphate limitation. *Plant J.* **6**, 673–685.

Battini, J.L., Rasko, J.E.J. and Miller, A.D. (1999) A human cell-surface receptor for xenotropic and polytropic murine leukemia viruses: possible role in G protein-coupled signal transduction. *Proc. Natl Acad. Sci. USA*, **96**, 1385–1390.

Borevitz, J.O., Xia, Y.J., Blount, J., Dixon, R.A. and Lamb, C. (2000) Activation tagging identifies a conserved MYB regulator of phenylpropanoid biosynthesis. *Plant Cell*, **12**, 2383–2393.

Chen, Z.H., Nimmo, G.A., Jenkins, G.I. and Nimmo, H.G. (2007) BHLH32 modulates several biochemical and morphological processes that respond to Pi starvation in Arabidopsis. *Biochem. J.* **405**, 191–198.

Chiou, T.J., Aung, K., Lin, S.I., Wu, C.C., Chiang, S.F. and Su, C.L. (2006) Regulation of phosphate homeostasis by microRNA in Arabidopsis. *Plant Cell*, **18**, 412–421.

Clough, S.J. and Bent, A.F. (1998) Floral dip: a simplified method for *Agrobacterium*-mediated transformation of *Arabidopsis thaliana*. *Plant J.* **16**, 735–743.

Delhaize, E. and Randall, P. (1995) Characterization of a phosphate-accumulator mutant of *Arabidopsis thaliana*. *Plant Physiol.* **107**, 207–213.

Devaiah, B.N., Nagarajan, V.K. and Raghothama, K.G. (2007a) Phosphate homeostasis and root development in Arabidopsis is synchronized by the zinc finger transcription factor ZAT6. *Plant Physiol.* **145**, 147–159.

Devaiah, B.N., Karthikeyan, A.S. and Raghothama, K.G. (2007b) WRKY75 transcription factor is a modulator of phosphate acquisition and root development in Arabidopsis. *Plant Physiol.* **143**, 1789–1801.

Fujii, H., Chiou, T.J., Lin, S.I., Aung, K. and Zhu, J.K. (2005) A miRNA involved in phosphate-starvation response in Arabidopsis. *Curr. Biol.* **15**, 2038–2043.

Hamburger, D., Rezzonico, E., MacDonald-Comber Petétot, J., Somerville, C. and Poirier, Y. (2002) Identification and character-

ization of the Arabidopsis PHO1 gene involved in phosphate loading to the xylem. *Plant Cell*, **14**, 889–902.

Jefferson, R.D., Kavanagh, T.A. and Bevan, M.W. (1987) GUS fusions: β-glucuronidase as a sensitive and versatile gene fusion marker in higher plants. *EMBO J.* **6**, 3901–3907.

Kang, X. and Ni, M. (2006) Arabidopsis SHORT HYPOCOTYL UNDER BLUE1 contains SPX and EXS domains and acts in cryptochrome signaling. *Plant Cell*, **18**, 921–934.

Lenburg, M.E. and O'Shea, E.K. (1996) Signaling phosphate starvation. *Trends Biochem. Sci.* **21**, 383–387.

Ma, Z., Bielenberg, D.G., Brown, K.M. and Lynch, J.P. (2001) Regulation of root hair density by phosphorus availability in *Arabidopsis thaliana*. *Plant Cell Environ.* **24**, 459–467.

Martin, A.C., del Pozo, J.C., Iglesias, J., Rubio, V., Solano, R., De La Pena, A., Leyva, A. and Paz-Ares, J. (2000) Influence of cytokinins on the expression of phosphate starvation responsive genes in Arabidopsis. *Plant J.* **24**, 559–567.

Miura, K., Rus, A., Sharkhuu, A. *et al.* (2005) The Arabidopsis SUMO E3 ligase SIZ1 controls phosphate deficiency responses. *Proc. Natl Acad. Sci. USA*, **102**, 7760–7765.

Mouillon, J.M. and Persson, B.L. (2006) New aspects on phosphate sensing and signalling in *Saccharomyces cerevisiae*. *FEMS Yeast Res.* **6**, 171–176.

Mudge, S.R., Rae, A.L., Diatloff, E. and Smith, F.W. (2002) Expression analysis suggests novel roles for members of the Pht1 family of phosphate transporters in Arabidopsis. *Plant J.* **31**, 341–353.

Mukatira, U.T., Liu, C., Varadarajan, D.K. and Raghothama, K.G. (2001) Negative regulation of phosphate starvation-induced genes. *Plant Physiol.* **127**, 1854–1862.

Nagata, T., Todoriki, S., Masumizu, T., Suda, I., Furuta, S., Du, Z. and Kikuchi, S. (2003) Levels of active oxygen species are controlled by ascorbic acid and anthocyanin in Arabidopsis. *J. Agric. Food Chem.* **51**, 2992–2999.

Nakanishi, H., Okumura, N., Umehara, Y., Nishizawa, N.K., Chino, M. and Mori, S. (1993) Expression of a gene specific for iron deficiency (Ids3) in the roots of *Hordeum vulgare*. *Plant Cell Physiol.* **34**, 401–410.

Olczak, M., Morawiecka, B. and Watorek, W. (2003) Plant purple acid phosphatases – genes, structures and biological function. 32 *Acta Biochim. Pol.* **50**, 1245–1256.

Pinson, B., Merle, M., Franconi, J.M. and Daignan-Fornier, B. (2004) Low affinity orthophosphate carriers regulate PHO gene expression independently of internal orthophosphate concentration in *Saccharomyces cerevisiae*. *J. Biol. Chem.* **279**, 35273–35280.

Poirier, Y. and Bucher, M. (2002) Phosphate transport and homeostasis in Arabidopsis. In *The Arabidopsis Book* (Somerville, C.R. and Meyerowitz, E.M., eds). Rockville, MD: American Society of Plant Biologists, doi:10.1199/tab.0024 (http://www.aspb.org/ 33 publications/arabidopsis/).

Poirier, Y., Thoma, S., Somerville, C. and Schiefelbein, J. (1991) A mutant of Arabidopsis deficient in xylem loading of phosphate. *Plant Physiol.* **97**, 1087–1093.

del Pozo, J.C., Allona, I., Rubio, V., Leyva, A., de la Pena, A., Aragoncillo, C. and Paz-Ares, J. (1999) A type 5 acid phosphatase gene from *Arabidopsis thaliana* is induced by phosphate starvation and by some other types of phosphate mobilizing/oxidative stress conditions. *Plant J.* **19**, 579–589.

Rubio, V., Linhares, F., Solano, R., Martin, A.C., Iglesias, J., Leyva, A. and Paz-Ares, J. (2001) A conserved MYB transcription factor involved in phosphate starvation signaling both in vascular plants and in unicellular algae. *Genes Dev.* **15**, 2122–2133.

Sell, S. and Hehl, R. (2005) A fifth member of the tomato 1-aminocyclopropane-1-carboxylic acid (ACC) oxidase gene family harbours a leucine zipper and is anaerobically induced. *DNA Seq.* **16**, 80–82.

Sheen, J. (2001) Signal transduction in maize and Arabidopsis mesophyll protoplasts. *Plant Physiol.* **127**, 1466–1475.

Shin, H., Shin, H.S., Chen, R. and Harrison, M.J. (2006) Loss of At4 function impacts phosphate distribution between the roots and the shoots during phosphate starvation. *Plant J.* **45**, 712–726.

Spain, B.H., Koo, D., Ramakrishnan, M., Dzudzor, B. and Colicelli, J. (1995) Truncated forms of a novel yeast protein suppress the lethality of a G protein a subunit deficiency by interacting with the b subunit. *J. Biol. Chem.* **270**, 25435–25444.

Ticconi, C.A., Delatorre, C.A., Lahner, B., Salt, D.E. and Abel, S. (2004) Arabidopsis *pdr2* reveals a phosphate-sensitive checkpoint in root development. *Plant J.* **37**, 801–814.

Varagona, M.J., Schmidt, R.J. and Raikhel, N.V. (1992) Nuclear localization signal(s) required for nuclear targeting of the maize regulatory protein Opaque-2. *Plant Cell*, **4**, 1213–1227.

Wang, Y., Ribot, C., Rezzonico, E. and Poirier, Y. (2004) Structure and expression profile of the Arabidopsis PHO1 gene family indicates a broad role in inorganic phosphate homeostasis. *Plant Physiol.* **135**, 400–411.

Author Query Form

Journal: TPJ

Article: 3460

Dear Author,
During the copy-editing of your paper, the following queries arose. Please respond to these by marking up your proofs with the necessary changes/additions. Please write your answers on the query sheet if there is insufficient space on the page proofs. Please write clearly and follow the conventions shown on the attached corrections sheet. If returning the proof by fax do not write too close to the paper's edge. Please remember that illegible mark-ups may delay publication.

Many thanks for your assistance.

Query reference	Query	Remarks
Q1	Au: Please check carefully throughout with respect to use of italics for all genes and non-italics for their respective proteins.	
Q2	Au: Please check amendment.	
Q3	Au: Please check amendment.	
Q4	Au: Please check sense. Why do its properties determine its low bioavailability?	
Q5	Au: Please check amendment/sense.	
Q6	Au: Please check insertion. Is it the gene itself that interacts or its product?	
Q7	Au: Please check nomenclature.	
Q8	Au: Please check amendments. Do they have conservative regions of other (non-Pfam-A) types?	
Q9	Au: Please check sense.	
Q10	Au: Please check sense. Sentence above also mentions first two exons – please avoid repetition.	
Q11	Au: Please clarify what these are.	
Q12	Au: Please check amendments, and also check concentrations of P_i (the words 'sensitively', 'while' and 'only' were deleted as they appeared to contradict the sense based on the concentrations given).	
Q13	Au: Please check amendments.	
Q14	Au: Please check amendments.	
Q15	Au: Please check sense.	

SPX domain is correct

Q2: It is OK

Q3: it is Ok

Q4: properties of phosphate

Q5: it is OK

Q16	Au: Please check amendment (or do you man that the AtSPX3-repressed plants show impaired growth?).
Q17	Au: Please check amendment.
Q18	Au: Please check amendment.
Q19	Au: Please check sense.
Q20	Au: Please check amendment/sense.
Q21	Au: Please check amendments.
Q22	Au: Please check amendment.
Q23	Au: Please give company URL.
Q24	Au: Please give company URL.
Q25	Au: Please check nomenclature and clarify what this is.
Q26	Au: Please define PEG.
Q27	Au: Please give company URL.
Q28	Au: Why are these partially lower-case and partially capitals?
Q29	Au: Please give supplier and URL.
Q30	Au: Please give department and town.
Q31	Au: Note that full legends will appear online, but only brief legends appear in print.
Q32	Au: Please check journal abbreviation.
Q33	Au: Please confirm that this is the title of the 'chapter'.
Q34	Au: What is it that is less conservative?
Q35	Au: Jeanmougin and Thompson, 1998 not found in the list. Please provide publication details.
Q36	Au: This part is marked 'C' in the figure, and there is another part 'B' that is not described here. Please amend legend or provide new artwork.
Q37	Au: Please provide an overall heading for this figure.
Q38	Au: Please provide an overall heading for this figure.
Q39	Au: Please check sense/clarify.

MARKED PROOF

Please correct and return this set

Please use the proof correction marks shown below for all alterations and corrections. If you wish to return your proof by fax you should ensure that all amendments are written clearly in dark ink and are made well within the page margins.

Instruction to printer	*Textual mark*	*Marginal mark*
Leave unchanged	··· under matter to remain	New matter followed by ⌐ or ⌐(x2)
Insert in text the matter indicated in the margin	⌐	
Delete	/ through single character, rule or underline or ⊢⊣ through all characters to be deleted	⌐/ or ⌐/(x2)
Substitute character or substitute part of one or more word(s)	/ through letter or ⊢⊣ through characters	new character / or new characters /
Change to italics	— under matter to be changed	⌐
Change to capitals	≡ under matter to be changed	≡
Change to small capitals	= under matter to be changed	=
Change to bold type	~ under matter to be changed	~
Change to bold italic	≈ under matter to be changed	≈
Change to lower case	Encircle matter to be changed	≠
Change italic to upright type	(As above)	⌐
Change bold to non-bold type	(As above)	⌐
Insert 'superior' character	/ through character or ⌐ where required	Y or Y under character e.g. Y^{3} or Y^{3}
Insert 'inferior' character	(As above)	⌐ over character e.g. Y_{2}
Insert full stop	(As above)	⊙
Insert comma	(As above)	,
Insert single quotation marks	(As above)	Y or Y and/or Y or Y
Insert double quotation marks	(As above)	Y or Y and/or Y or Y
Insert hyphen	(As above)	⊢
Start new paragraph	⌐	⌐
No new paragraph	⌐	⌐
Transpose	⌐	⌐
Close up	linking ⁀ characters	⁀
Insert or substitute space between characters or words	/ through character or ⌐ where required	Y
Reduce space between characters or words	| between characters or words affected	⊤